
This is an electronic reprint of the original article.
This reprint may differ from the original in pagination and typographic detail.

Nieminen, Heikki J.; Laidmäe, Ivo; Salmi, Ari; Rauhala, Timo; Paulin, Tor; Heinämäki, Jyrki; Hæggström, Edward

Ultrasound-enhanced electrospinning

Published in:
Scientific Reports

DOI:
[10.1038/s41598-018-22124-z](https://doi.org/10.1038/s41598-018-22124-z)

Published: 01/12/2018

Document Version
Publisher's PDF, also known as Version of record

Published under the following license:
CC BY

Please cite the original version:
Nieminen, H. J., Laidmäe, I., Salmi, A., Rauhala, T., Paulin, T., Heinämäki, J., & Hæggström, E. (2018). Ultrasound-enhanced electrospinning. *Scientific Reports*, 8(1), 1-6. Article 4437. <https://doi.org/10.1038/s41598-018-22124-z>

SCIENTIFIC REPORTS

OPEN

Ultrasound-enhanced electrospinning

Heikki J. Nieminen^{1,2}, Ivo Laidmäe^{3,4}, Ari Salmi¹, Timo Rauhala¹, Tor Paulin¹, Jyrki Heinämäki³ & Edward Hægström¹

Received: 22 June 2017

Accepted: 13 February 2018

Published online: 13 March 2018

Electrospinning is commonly used to produce polymeric nanofibers. Potential applications for such fibers include novel drug delivery systems, tissue engineering scaffolds, and filters. Electrospinning, however, has shortcomings such as needle clogging and limited ability to control the fiber-properties in a non-chemical manner. This study reports on an orifice-less technique that employs high-intensity focused ultrasound, *i.e.* ultrasound-enhanced electrospinning. Ultrasound bursts were used to generate a liquid protrusion with a Taylor cone from the surface of a polymer solution of polyethylene oxide. When the polymer was charged with a high negative voltage, nanofibers jetted off from the tip of the protrusion landed on an electrically grounded target held at a constant distance from the tip. Controlling the ultrasound characteristics permitted physical modification of the nanofiber topography at will without using supplemental chemical intervention. Possible applications of tailor-made fibers generated by ultrasound-enhanced electrospinning include pharmaceutical controlled-release applications and biomedical scaffolds with spatial gradients in fiber thickness and mechanical properties.

Electrospinning (ES) is nanotechnology that employs an electric field to pull nanofibers from a polymer solution. A Taylor cone^{1,2} is formed at the surface of the polymer solution extrusion, typically charged with high voltage (several -kV), and it serves as the location of the ejection of an initial fiber. The final fiber is typically formed through a drying process. The product is collected onto a charged collector by electric attraction (typically higher potential than at the polymer, *e.g.* ground or positive potential). Different implementations of ES exist featuring different potentials at the source polymer and target³.

In conventional ES, fiber ejection typically takes place from a small polymer droplet located at an orifice, *e.g.* at a tip of a charged needle. The droplet is refilled by pumping new polymer solution to the needle tip through the needle. This is widely used approach, but is limited by needle clogging issues⁴, and rapid control of fiber properties during an ES event has not been reported. Clogging can be overcome with orifice-less approaches^{5–12}. However, changing the fiber-properties (*e.g.* the diameter) rapidly during ES is limited to changing common ES parameters¹³, the distance between the Taylor cone and the collector¹⁴, the environment^{15,16}, nozzle diameter¹⁷, polymer solution properties^{18,19}, and solution feed-rate²⁰. All these approaches are impractical and limit the spatiotemporal control. Sub-second modulation of fiber the diameter could permit generating layer-by-layer fibers with different thickness/shape properties. This could potentially enable gradients in fiber constructs, for purposes such as (i) controlled drug release systems, (ii) tissue engineering scaffolds, and (iii) filters.

High-intensity focused ultrasound (HIFU) provides a means to actuate matter. In practice, ultrasound (US) with high intensity can be used to push or palpate material and material interfaces using acoustic radiation pressure²¹. At interfaces between gas, liquid, and solid, US can generate radiation forces that push the boundary. In a configuration, where US travels through liquid to a liquid-gas interface (*e.g.* polymer solution-air -interface), a localized impingement of US on this acoustic interface creates a protrusion at the liquid surface. Inside fluids, a travelling US wave can generate acoustic streaming along the direction of sound propagation²². In conjunction with bubbles, US can make micro/nano-bubbles oscillate and, contribute to rapid streaming^{23,24} and fluid micro-jets at micron scale^{25,26}. HIFU can also heat a material within a confined volume, *e.g.* within “ultrasonic

¹Electronics Research Laboratory, Department of Physics, University of Helsinki, Helsinki, Finland. ²Medical Ultrasonics Laboratory (MEDUSA), Department of Neuroscience and Biomedical Engineering, Aalto University, Espoo, Finland. ³Institute of Pharmacy, University of Tartu, Tartu, Estonia. ⁴Department of Immunology, Institute of Biomedicine and Translational Medicine, University of Tartu, Tartu, Estonia. Heikki J. Nieminen and Ivo Laidmäe contributed equally to this work. Correspondence and requests for materials should be addressed to H.J.N. (email: heikki.j.nieminen@aalto.fi)

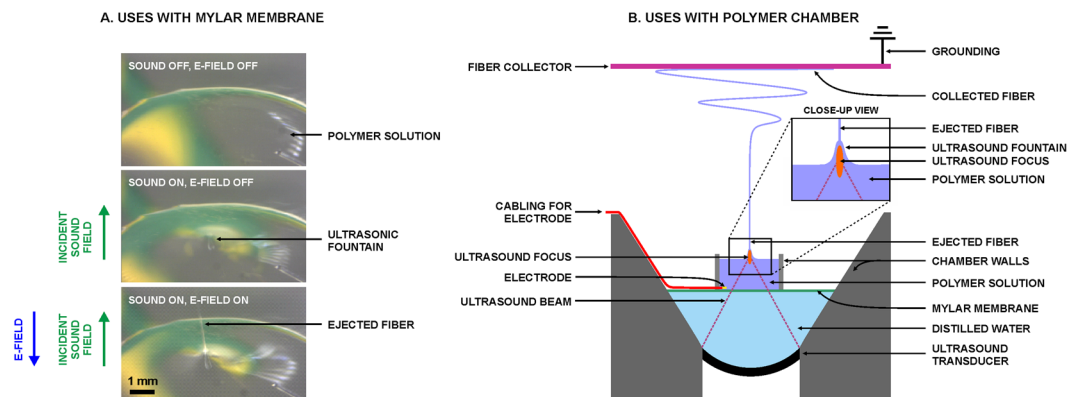


Figure 1. (A) The applied high-intensity ultrasound generated an acoustic fountain, when a polymer droplet was placed on a 0.2-mm thick mylar membrane (acoustically conducting, but electrically isolating), while focusing the beam through water at the polymer-air interface. When the polymer was charged using an electrode (from -5 kV to -15 kV) and an electrically grounded target was placed above the fountain, a liquid jet was observed at the top of the ultrasonic fountain. (B) The method described in (A) was developed into a USES system, which was employed for systematic investigation of ultrasonic fiber-topography control using an -11.3 kV electrode voltage and 15 cm polymer to target distance.

fountains” generated at liquid interface²⁷, induced by acoustic radiation force. While US-matter interactions are many, their exploitation to manipulate the electrospun fiber during ES has been overlooked in the literature.

To date, US in conjunction with ES, has not been systematically investigated as a means to modify the topography or diameter of nanospun fibers. This study aims to (i) to establish an orifice-less ES system based on acoustic radiation pressure, and (ii) to explore the technique’s potential to modify the topography of polyethylene oxide (PEO) nanofibers.

Results

The ultrasound-enhanced electrospinning (USES) method (Fig. 1A) and a system (Fig. 1B) were successfully established. High-intensity US was generated by a focused piezo-ceramic transducer. The US beam (focus width = 1.0 mm, focus length = 6.9 mm at -3 dB of peak-positive-pressure) was directed through a 0.2-mm thick mylar membrane (beam axis perpendicular to the mylar membrane; the membrane is acoustically conducting, but electrically isolating) to a location within an open chamber carrying the source polymer solution (Fig. 1B). The space between the membrane and transducer was filled with purified water to conduct sound from the transducer to the target polymer. When the polymer-air -interface level was vertically adjusted to coincide with the US focus, a visible protrusion of polymer (“ultrasonic fountain”) with a height up to few millimeters was observed for specific ultrasonic parameters (time-averaged total acoustic power, *i.e.* TAP = low: 0.3 W; medium: 1.0 W; high: 1.4 W; frequency = 2.16 MHz; pulse repetition frequency, *i.e.* PRF = 150; duty cycle = 1.7%). When an electrode inside the polymer chamber, but outside the US beam, was charged (-11.3 kV), vertical ejection of polymer was visually observed from the tip of the protrusion. The ejected fibers were collected on an aluminium foil target, which was electrically grounded and positioned horizontally 15 cm above the polymer solution surface.

USES provided means to produce stable nano-fiber production. Repeatedly, the produced nanofiber constructs were visually the same, when same TAP was applied. Low (TAP = 0.3 W) and medium (TAP = 1.0 W) US power produced on average thicker fibers than those produced with the high US power setting (Fig. 2). The ‘medium’ and ‘high’ power as well as the reference method (conventional ES) produced more beads (ellipsoidal or round thickenings within the fiber constructs) than the ‘low’ power setting (Fig. 2).

Quantitative analysis of the fibers in a test/re-test -experiment demonstrated that on average the thinnest fibers were produced with the reference method (178 ± 64 nm; mean \pm S.D; $n = 150$) and repeated with USES using the ‘high’ US power setting (test: 205 ± 60 nm, $n = 150$; re-test: 233 ± 65 nm, $n = 150$; mean of the two tests = 219 nm) (Fig. 2, right). The average fiber diameters for both medium and low US power settings were on average higher (medium; test: 280 ± 82 nm, $n = 150$; re-test: 290 ± 77 nm; mean of the two tests = 285 nm; Low; test: 312 ± 43 nm, $n = 150$; re-test: 298 ± 48 nm, $n = 150$; mean of the two tests = 305 nm) (Fig. 2, right). The fiber diameters in each setting group differed statistically significantly: low-mid, $p = 0.0182$; low-high, $p < 0.0001$, mid-high, $p < 0.0001$. The fiber diameters in each setting group also differed from fiber diameters in reference group (ES-generated fibers) ($p < 0.0001$).

Discussion

The new orifice-less US-enhanced ES method, USES, was successfully established in this study. USES demonstrated capability to generate polymeric nanofibers, whose properties were associated with the applied US settings in a repeatable manner. The data in this manuscript was generated from spinning events that lasted 38 to 60 seconds. However, the method permitted successful spinning for hours, when a capillary was connected to the source polymer chamber to continuously re-fill the polymer chamber with PEO. In this arrangement, the feed-rate was up to 3 mL/h, which is $3 \times$ compared to the feed-rate 1 mL/h of the conventional ES.

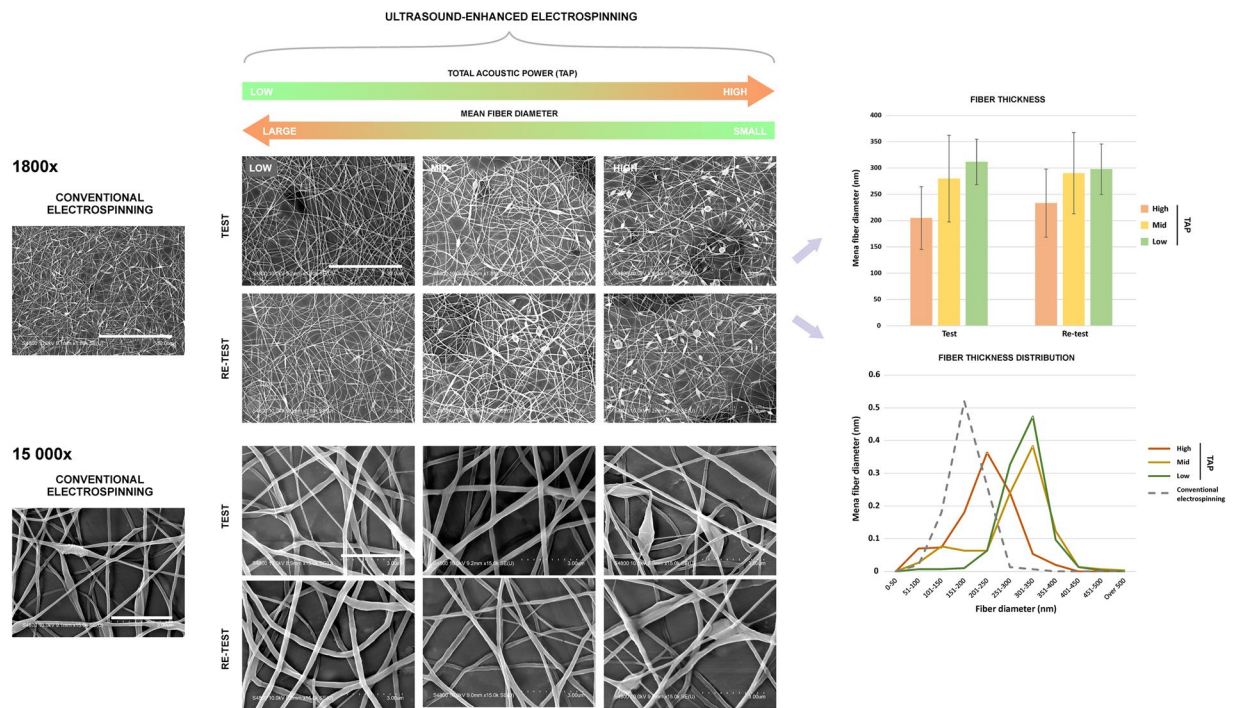


Figure 2. Left and center: Scanning electron microscope images of fibers produced with the ultrasound-enhanced electrospinning (USES) device at low, mid and high ultrasonic power. Top row corresponds to the test and the lower row to a re-test. Low ultrasonic power exhibited fibers with minor “beading”, whereas beading was most pronounced in fibers generated with high ultrasound power and with the reference technique (conventional electrospinning). The images suggest that the visual appearance of fibers was similar in the test compared to the re-test. Ultrasonically enhanced fibers appear thicker than those produced with the reference method. The results suggest that the appearance of the topography of fibers generated with USES can be repeatedly modified. Right: Distribution of fiber diameters produced at high, mid or low ultrasound power in test/re-test -experiments. All methods produced nanofibers with 50–500 nm diameter. Ultrasound-enhanced fibers were qualitatively thicker and statistically different in diameter ($p < 0.0001$) than those produced with the reference method. The fibers produced using high ultrasound power were qualitatively thinner and statistically significantly different ($p < 0.0001$) than those produced with ‘mid’ or ‘low’ ultrasound power. The ‘mid’ ultrasound exposure produced a narrower fiber distribution than the low power, but low power produce thinner fibers in the 50–200 nm range. The results suggest that the distribution in fiber diameter can be modified by changing the ultrasound power, without changing the chemical composition of the source polymer. The reference fibers were produced with conventional needle electrospinning. For comparability the area of each histogram was normalized to 1. For statistical analysis, non-parametric Kruskal-Wallis for pairwise comparison with Bonferroni adjustment was used. Scale bars for 1800 \times and 15 000 \times magnifications corresponds to 30 μm and 3 μm , respectively.

Interestingly, the mean fiber diameter decreases with increasing TAP (Fig. 2, right). The distribution of fiber diameters is also affected by the applied ultrasonic settings (Fig. 2, right) and the groups differed statistically. It appears that the fibers generated with USES are thicker than those generated with conventional ES using the same polymer solution.

Several phenomena may take place at the proximity of the ultrasonic fountain, and may be associated with the demonstrated control of fiber properties:

1. Acoustic radiation force²¹ in conjunction with the electric field^{1,2}
2. Capillary waves at the surface of the polymer generated by US^{28,29}
3. Cavitation^{23–25,28},
4. Acoustic streaming²²
5. Thermal effects²⁷.

Since the (i) ultrasonic fountain generation is reported in the literature^{28,30}, and since (ii) fiber generation was impossible without the ultrasonic fountain, and since (iii) fiber ejection was observed at the tip of the fountain, the acoustic radiation force plays a fundamental role in determining where the fiber generation occurs. The electric field density typically concentrates at material extrusions; therefore, it is expected to concentrate also at the tip of the fountain. In our experience, if US settings with visible acoustic streaming were used, the sharpness of the protrusion was compromised, which prevented spinning from starting. Spinning occurred, when the protrusion was narrow, i.e. ~ 1 mm in diameter or less.

Interestingly, the fibers generated with ES using the same polymer were on average smaller in diameter compared to those generated with USES. One potential explanation for this is the self-focusing funnel-like shape of the ultrasonic fountain. This is expected to guide US waves towards the fiber and potentially into the fiber. This focusing may, therefore, induce upwards momentum also in the fiber in addition to that momentum generated by the electric field. This addition would enhance mass transfer, as suggested by the higher feed-rate (up to 3 mL/h) compared to ES (1 mL/h), and, thus, produces thicker fibers. Moreover, temperatures at ultrasonic fountains can be high due to high ultrasonic intensities²⁷; therefore, thermal effects are expected to contribute to *e.g.* the drying process of the fiber and possibly to modification of the polymer structure. Ultrasound has also been reported to be able to modify the polymer viscosity or conductivity^{11,31}. Further investigations specifically for each polymer-drug-combination, would be deemed, because of potential damage to the molecule or polymer that could affect the drug activity.

In our experiments, the initiation of ES from the ultrasonic fountain strongly depended on the pulse repetition frequency (PRF). Typically, ES initiation occurred for 100–200 Hz PRF; the empirical optimum PRF was 150 Hz for PEO (3% w/v). Moreover, for ES using lowest TAP setting (generates a smaller fountain than with the mid or high TAP setting), higher TAP was initially required to initiate spinning. Once spinning began, the US settings could be changed, while maintaining fiber production even at low TAP.

The possible applications of USES-generated fibers are many. In the following we discuss two applications that we find prominent.

1. Electrospun fibers are investigated as possible means to modify drug release, especially poorly water-soluble ones. The fiber diameter is associated with the total active surface area per unit mass. Thin fibers release drugs faster than thick fibers³². Therefore, the capability to modify fiber diameter by physical means provides potentially a way to tailor drug release properties within the same fiber construct non-chemically, even though it was not demonstrated in this study. This would be a great advantage compared to the state-of-the-art, which typically requires the chemical modification of the polymer solution (*i.e.* changing concentration or nature of the polymer) of the polymer solution to modify fiber properties such as topography and diameter.
2. Electrospun fibers are widely used to produce scaffolds for tissue engineering purposes³³. Tissue engineering using *e.g.* stem cells differentiate by reacting to their mechanical environment^{33,34}. A scaffold with gradients in fiber construct properties should influence the mechanical environment the cells are embedded in^{33,35}; therefore, USES-induced gradients in fiber construct properties could provide unique means to produce tissue engineering scaffolds with gradients in mechanical properties simply by changing the US parameters during the spinning process.

The literature reports on several orifice-less ES techniques^{5–10}. Unfortunately, none of the available approaches have been reported to be capable of controlling fiber topography or diameter spatiotemporally in a time-frame of a second. Therefore, USES is a significant improvement over the pre-existing methods. Moreover, USES can be scaled up: (i) one can multiply the number of transducers and ES jets; or (ii) a transducer array can be used to electronically steer the focus to several positions on a polymer surface to induce several ultrasonic fountains with several locations of fiber ejection within a single source polymer chamber.

To conclude, we established a new orifice-less ES platform that features US enhancement. USES provides physical means to control polymeric fiber topography in PEO and diameter without supplementary chemical intervention. It also solves clogging issues associated with conventional ES approaches. USES could be scaled up if found feasible for industrial use. Possible applications include, but are not limited to, tailored drug delivery systems and tissue engineering scaffolds with gradients.

Materials and Methods

Experimental system. An ES setup illustrated in Fig. 1B was established. The US transducers were electrically grounded from its top surface and charged from its bottom surface with a driving voltage. The signal driving the piezoceramic transducer (radius of curvature = 29 mm, outer diameter = 29 mm) was provided by a signal generator and a power amplifier (500A100A, Amplifier Research Corp., Souderton, PA). A high voltage supply (P3067D; Kevex Instruments, San Carlos, CA) was used to charge the electrode within the polymer chamber (Fig. 1B).

Electrospinning. The solution for ES was PEO aqueous solution (3% w/v), prepared by overnight dissolving PEO (Average Mw 900,000; Sigma-Aldrich Inc., St. Louis, MO) into deionized water with agitation in ambient conditions. An in-house conventional ES system with a syringe, pump (KDS-230-CE; KD Scientific Inc., Holliston, MA) and a 23 G hypodermic needle, which served as the polymer feeding capillary (feeding rate was 1 ml/h), was used to produce reference nanofibers, otherwise with same settings as in USES.

Three different ultrasonic settings were used in the USES (see Results). Tests with different US settings were repeated twice with same settings, but with reversed order. Control fibers were generated with conventional ES. Fiber collection time was 38 sec to 1 min. Experiments were done in ambient conditions. To avoid influence of *e.g.* change in relative humidity all spinning experiments were done inside one hour. The samples for ES and USES were generated from the same starting aqueous PEO solution.

Scanning electron microscopy (SEM) and fiber analysis. From each test, two samples were selected for SEM analysis (S-4800 FE-SEM; Hitachi Ltd., Tokyo, Japan). The samples were attached to the sample holder with carbon tape (Carbon Conductive Double-faced Adhesive Tape; Nisshin EM Co. Ltd., Tokyo, Japan) followed by platinum-coating (6 nm) prior to SEM imaging with 1 800× and 15 000× magnifications (acceleration

voltage = 10 kV, emission current = 10 μ A). The diameters of nanofibers were measured using ImageJ 1.51 g software at random locations within the SEM images. The fiber diameter is presented as mean (\pm SD) of 150 individual measurements from each spinning event.

Statistical analysis. For comparison of fiber diameter distributions in the experimental groups, a non-parametric Kruskal-Wallis for pairwise comparison with Bonferroni adjustment was used. Statistical analysis was performed using the computing environment R (R version 3.4.0, R Development Core Team, 2017).

References

1. Taylor, G. Disintegration of water drops in an electric field. *Proc. Royal Soc. Lond. A*. **280**, 383–397 (1964).
2. Taylor, G. Electrically driven jets. *Proc. Royal Soc. Lond. A*. **313**, 453–475 (1969).
3. Teo, W. E. & Ramakrishna, S. A review on electrospinning design and nanofibre assemblies. *Nanotechnology* **17**, R89 (2006).
4. Kanjanapongkul, K., Wongsasulak, S. & Yoovidhya, T. Investigation and prevention of clogging during electrospinning of zein solution. *J. Appl. Polym. Sci.* **118**, 1821–1829 (2010).
5. Alamein, M. A. *et al.* Nanospiderwebs: artificial 3D extracellular matrix from nanofibers by novel clinical grade electrospinning for stem cell delivery. *Adv. Healthcare Mat.* **2**, 702–717 (2013).
6. Li, D. *et al.* Three-dimensional polycaprolactone scaffold via needleless electrospinning promotes cell proliferation and infiltration. *Colloids Surf. B Biointerfaces* **121**, 432–443 (2014).
7. Dosunmu, O., Chase, G. G., Kataphinan, W. & Reneker, D. Electrospinning of polymer nanofibres from multiple jets on a porous tubular surface. *Nanotechnology* **17**, 1123 (2006).
8. Varabhas, J., Chase, G. G. & Reneker, D. Electrospun nanofibers from a porous hollow tube. *Polymer* **49**, 4226–4229 (2008).
9. Huang, X., Wu, D., Zhu, Y. & Sun, D. Needleless electrospinning of multiple nanofibers. *Nanotechnology*, 7th IEEE Conference on Nanotechnology, 823–826 (2007).
10. Yarin, A. & Zussman, E. Upward needleless electrospinning of multiple nanofibers. *Polymer* **45**, 2977–2980 (2004).
11. Li, S. *et al.* Effect of ultrasonic vibration on the morphology of bubble-electrospun nanofibers. *Fiber. Polym.* **16**, 2432 (2015).
12. Liu, H. Y., Kong, H. Y., Wang, M. Z. & He, J. H. Lightning-like Charged Jet Cascade in Bubble Electrospinning with Ultrasonic Vibration **27**. *J. Nano Res.* 111–119 (2014).
13. Lee, J. S. *et al.* Role of molecular weight of atactic poly (vinyl alcohol)(PVA) in the structure and properties of PVA nanofabric prepared by electrospinning. *J. Appl. Pol. Sci.* **93**, 1638–1646 (2004).
14. Ding, W. *et al.* Manipulated electrospun PVA nanofibers with inexpensive salts. *Macromol. Mat. Eng.* **295**, 958–965 (2010).
15. Fashandi, H. & Karimi, M. Pore formation in polystyrene fiber by superimposing temperature and relative humidity of electrospinning atmosphere. *Polymer* **53**, 5832–5849 (2012).
16. Htike, H. H., Chen, L. & Sukigara, S. The Effect of Relative Humidity on Electrospinning of Poly-(vinyl alcohol) with Soluble Eggshell Membrane. *J. Textile Eng.* **58**, 9–12 (2012).
17. Heikkilä, P. & Harlin, A. Parameter study of electrospinning of polyamide-6. *Eur. Polymer J.* **44**, 3067–3079 (2008).
18. Tan, S., Inai, R., Kotaki, M. & Ramakrishna, S. Systematic parameter study for ultra-fine fiber fabrication via electrospinning process. *Polymer* **46**, 6128–6134 (2005).
19. Zong, X. *et al.* Structure and process relationship of electrospun bioabsorbable nanofiber membranes. *Polymer* **43**, 4403–4412 (2002).
20. Deitzel, J. M., Kleinmeyer, J., Harris, D. & Tan, N. B. The effect of processing variables on the morphology of electrospun nanofibers and textiles. *Polymer* **42**, 261–272 (2001).
21. Westervelt, P. J. The theory of steady forces caused by sound waves. *J. Acoust. Soc. Am.* **23**, 312–315 (1951).
22. Nyborg, W. L. Acoustic streaming due to attenuated plane waves. *J. Acoust. Soc. Am.* **25**, 68–75 (1953).
23. Cho, E., Chung, S. K. & Rhee, K. Streaming flow from ultrasound contrast agents by acoustic waves in a blood vessel model. *Ultrasonics* **62**, 66–74 (2015).
24. Liu, X. & Wu, J. Acoustic microstreaming around an isolated encapsulated microbubble. *J. Ac. Soc. Am.* **125**, 1319–1330 (2009).
25. Izadifar, Z., Babyn, P. & Chapman, D. Mechanical and Biological Effects of Ultrasound: A Review of Present Knowledge. *Ultrasound Med. Biol.* (2017).
26. Manmi, K. & Wang, Q. Acoustic microbubble dynamics with viscous effects. *Ultrason. Sonochem.* **36**, 427–436 (2017).
27. Tingaud, F., Ferrouillat, S., Colasson, S., Bontemps, A. & Bulliard-Sauret, O. Experimental characterisation of the thermal behaviour of different materials submitted to ultrasound in an ultrasonic fountain. *Ultrason. Sonochem.* **20**, 1046–1053 (2013).
28. Simon, J. C., Sapozhnikov, O. A., Khokhlova, V. A., Crum, L. A. & Bailey, M. R. Ultrasonic atomization of liquids in drop-chain acoustic fountains. *J. Fluid. Mech.* **766**, 129–146 (2015).
29. Mahravan, E., Naderan, H. & Damangir, E. Frequency and wavelength prediction of ultrasonic induced liquid surface waves. *Ultrasonics* **72**, 184–190 (2016).
30. Xu, Z., Yasuda, K. & Liu, X. Simulation of the formation and characteristics of ultrasonic fountain. *Ultrason. Sonochem.* **32**, 241–246 (2016).
31. Price, G., West, P. & Smith, P. Control of polymer structure using power ultrasound. *Ultrason. Sonochem.* **1**, S51–S57 (1994).
32. Chou, S.-F., Carson, D. & Woodrow, K. A. Current strategies for sustaining drug release from electrospun nanofibers. *J. Contr. Rel.* **220**, 584–591 (2015).
33. Ngadiman, N. H. A., Noordin, M., Idris, A. & Kurniawan, D. A review of evolution of electrospun tissue engineering scaffold: From two dimensions to three dimensions. *Proc. Inst. Mech. Eng. H.*, 0954411917699021 (2017).
34. Dado, D., Sagi, M., Levenberg, S. & Zemel, A. Mechanical control of stem cell differentiation. *Regen. Med.* **7**, 101–116 (2012).
35. Moroni, L., Licht, R., de Boer, J., de Wijn, J. R. & van Blitterswijk, C. A. Fiber diameter and texture of electrospun PEOT/PBT scaffolds influence human mesenchymal stem cell proliferation and morphology, and the release of incorporated compounds. *Biomaterials* **27**, 4911–4922 (2006).

Author Contributions

All authors contributed to planning, reviewing the data, and writing the manuscript. H.N., I.L., A.S., T.P. and T.R. contributed to running the experiments as well as to obtaining and analyzing the data.

Additional Information

Competing Interests: All authors are inventors in a patent application PCT/FI2016/050170.

Publisher's note: Springer Nature remains neutral with regard to jurisdictional claims in published maps and institutional affiliations.



Open Access This article is licensed under a Creative Commons Attribution 4.0 International License, which permits use, sharing, adaptation, distribution and reproduction in any medium or format, as long as you give appropriate credit to the original author(s) and the source, provide a link to the Creative Commons license, and indicate if changes were made. The images or other third party material in this article are included in the article's Creative Commons license, unless indicated otherwise in a credit line to the material. If material is not included in the article's Creative Commons license and your intended use is not permitted by statutory regulation or exceeds the permitted use, you will need to obtain permission directly from the copyright holder. To view a copy of this license, visit <http://creativecommons.org/licenses/by/4.0/>.

© The Author(s) 2018